Measuring CMB Polarization with BOOMERANG

T. Montroy[1,10], P.A.R. Ade[3], A. Balbi[18], J.J. Bock[4,16], J.R. Bond[5], J. Borrill[6,19], A. Boscaleri[7], P. Cabella[18], C.R. Contaldi[5], B.P. Crill[8], P. de Bernardis[2], G. De Gasperis[18], A. de Oliveira-Costa[14], G. De Troia[2], G. di Stefano[13], K. Ganga[9], E. Hivon[9], V.V. Hristov[16], A. Iacoangeli[2], A.H. Jaffe[17], T.S. Kisner[1,10], W.C. Jones[16], A.E. Lange[16], S. Masi[2], P.D. Mauskopf[3], C. MacTavish[15], A. Melchiorri[2], F. Nati[2], P. Natoli[18], C.B. Netterfield[15], E. Pascale[15], F. Piacentini[2], D. Pogosyan[11], G. Polenta[2], S. Prunet[12], S. Ricciardi[2], G. Romeo[13], J.E. Ruhl[1], E. Torbet[10], M. Tegmark[14], and N. Vittorio[18].

[1] *Physics Department, Case Western Reserve University, Cleveland, OH, USA*
[2] *Dipartimento di Fisica, Universitá di Roma La Sapienza, Roma, Italy*
[3] *Dept. of Physics and Astronomy, Cardiff University, Cardiff CF24 3YB, Wales, UK*
[4] *Jet Propulsion Laboratory, Pasadena, CA, USA*
[5] *Canadian Institute for Theoretical Astrophysics, University of Toronto, Toronto, Ontario, Canada*
[6] *National Energy Research Scientific Computing Center, LBNL, Berkeley, CA, USA*
[7] *IFAC-CNR, Firenze, Italy*
[8] *CSU Dominguez Hills, Carson, CA, USA*
[9] *IPAC, California Institute of Technology, Pasadena, CA, USA*
[10] *Dept. of Physics, University of California, Santa Barbara, CA, USA*
[11] *Physics Dept., University of Alberta, Edmonton, Alberta, Canada*
[12] *Institut d'Astrophysique, Paris, France*
[13] *Istituto Nazionale di Geofisica, Roma, Italy*
[14] *Physics Department, University of Pennsylvania, Philadelphia, PA, USA*
[15] *Physics Department, University of Toronto, Toronto, Ontario, Canada*
[16] *Observational Cosmology, California Institute of Technology, Pasadena, CA, USA*
[17] *Astrophysics Group, Imperial College, London, UK*
[18] *Dipartimento di Fisica, Universitá di Roma Tor Vergata, Roma, Italy*
[19] *Center for Particle Astrophysics, University of California, Berkeley, CA, USA*

ABSTRACT

BOOMERANG is a balloon-borne telescope designed for long duration (LDB) flights around Antarctica. The second LDB Flight of BOOMERANG took place in January 2003. The primary goal of this flight was to measure the polarization of the CMB. The receiver uses polarization sensitive bolometers at 145 GHz. Polarizing grids provide polarization sensitivity at 245 and 345 GHz. We describe the BOOMERANG telescope noting changes made for 2003 LDB flight, and discuss some of the issues involved in the measurement of polarization with bolometers. Lastly, we report on the 2003 flight and provide an estimate of the expected results.

1. Introduction

The 1998 flight of BOOMERANG (B98) provided a measurement of the angular power spectrum of CMB temperature anisotropies from $\ell = 25$ to $\ell = 1000$ (Ruhl et al. 2002). BOOMERANG made its second long duration balloon (LDB) flight (BOOM03) in January 2003 with a receiver configured to simultaneously measure CMB temperature and polarization anisotropies. The new receiver used pairs of polarization sensitive bolometers (PSB's) at 145 GHz. At 245 GHz and 345 GHz, spider web bolometers are used with polarization sensitivity provided by polarizing grids mounted at the front of the cryogenic feed horns. The B98 results were partially limited by pointing reconstruction error ($2.5'$ rms). For the BOOM03 flight, we added a pointed sun sensor and a tracking star camera which should reduce our pointing reconstruction error to less than $1'$ rms. From the BOOM03 flight, we have 11.7 days of data. An analysis effort is underway, with the goal of producing measurements of C_ℓ^T, C_ℓ^{TE} and C_ℓ^{EE}.

2. Telescope

The BOOMERANG telescope (Figure 1) was designed specifically for the harsh conditions of Antarctic ballooning (Crill et al. 2002). The extensive shielding prevents the contamination by stray-light, and protects other sensitive components from the Sun. This is especially important for daytime ballooning over Antarctica, where thermal management is vital. The back of the telescope is constantly illuminated by the Sun, reaching temperatures of 55° C, while the front is shaded and can cool to less than −20° C.

BOOMERANG scans in azimuth, with the elevation kept constant for at least one hour. Sky rotation turns this one-dimensional azimuthal scan strategy into a cross-linked pattern on the celestial sphere. B98 and BOOM03 both used a differential GPS array, a fixed Sun sensor and rate gyros for pointing reconstruction. For BOOM03, the pointed sun sensor and tracking star camera should improve the pointing reconstruction error.

The BOOMERANG primary mirror is an off-axis parabola with a diameter of 1.3 m. It is 45° degrees off axis and has a focal length of 1280 mm. The primary feeds a pair of cold re-imaging mirrors which are kept at 1.65 K inside the cryostat (Figure 2). The tertiary forms an image of the primary and acts as the Lyot stop for our system. It controls the illumination on the primary, limiting the effective diameter to about 80 cm. There is a 1 cm hole in the tertiary behind which sits a calibration lamp. It fires once every 15 minutes allowing us to monitor any calibration drift.

The BOOMERANG cryostat can keep the detectors at 0.275 K for 15 days (Masi et al. 1999). Toroidal nitrogen and helium tanks (with the helium tank inside the nitrogen tank) are suspended via 1.6 mm Kevlar ropes. The insert, which contains the cold mirrors and the focal plane, is bolted to the helium tank. The insert also contains a single stage ^{3}He refrigerator which can keep the focal plane at 0.275 K for 12-13 days (Masi et al. 1999). Since the ^{4}He and LN_2 stages have a longer hold time (18 and 16 days respectively) than the ^{3}He stage, we added capability for an in-flight cycle of the ^{3}He refrigerator.

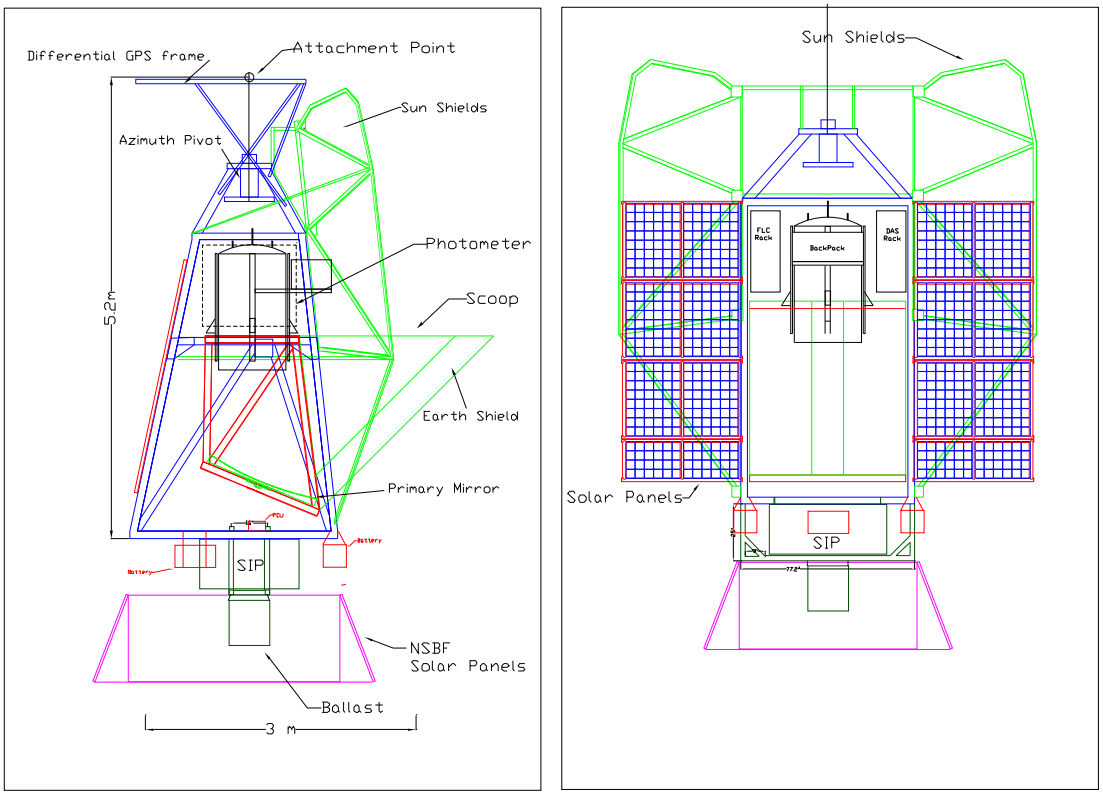

Fig. 1.— The BOOMERANG payload. The extensive shielding prevents stray-light contamination and helps to maintain thermal stability.

3. BOOM03 Receiver

The BOOM03 receiver was designed for measurement of CMB temperature and polarization anisotropies. There are 8 pixels, and each pixel contains two detectors. Four of the pixels contain pairs of polarization sensitive bolometers (PSB's) operating at 145 GHz. The other four pixels are 2-color photometers operating at 245 and 345 GHz. Both the PSB's and the photometers use corrugated feed horns. Table 1 summarizes the properties of the BOOM03 receiver. Figure 3 shows the layout of the focal plane projected onto the sky.

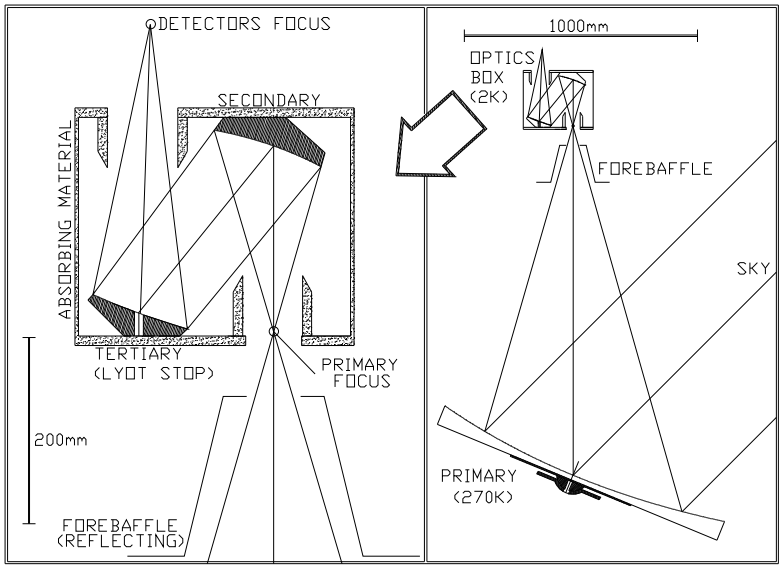

Fig. 2.— An overview of the BOOMERANG optics. Radiation from the primary reflects off the secondary, to the tertiary and then to the focal plane. The secondary and tertiary correct aberrations induced by the primary. They are kept at 1.65 K in a box coated with absorbing material. The tertiary acts as the Lyot stop for the system, controlling the illumination of the primary. Spillover off the edge of the tertiary sees a 1.65 K blackbody.

Freq	Bandwidth	#Channels	Beam FWHM	Exp. NET$_{CMB}$
145 GHz	46 GHz	8	$9.5'$	160 $\mu K\sqrt{s}$
245 GHz	100 GHz	4	$6.5'$	290 $\mu K\sqrt{s}$
345 GHz	100 GHz	4	$7'$	660 $\mu K\sqrt{s}$

Table 1: Summary of the properties of the BOOM03 receiver. The FWHM is based on a pre-flight measurement using a tethered thermal source placed 1 km from the telescope. The NET_{CMB} is calculated using a model of our detectors based on pre-flight loadcurve data. Preliminary analysis of flight data provides a similar answer at 145 GHz

3.1. Polarization Sensitive Bolometers

The polarization sensitive bolometers are a variation on the original micro-mesh design used in B98 (Jones et al. 2003). Instead of a spider web design, the mesh is a square grid. The grid is only metallized in one direction (Figure 4) making it sensitive to only one component of the incoming electric field. A pair of these with metallized directions oriented 90° apart are mounted at the end of a corrugated feed structure, separated by 60μm along the axis of propagation. This allows for simultaneous measurement of both electric field components at the same point on the sky, through

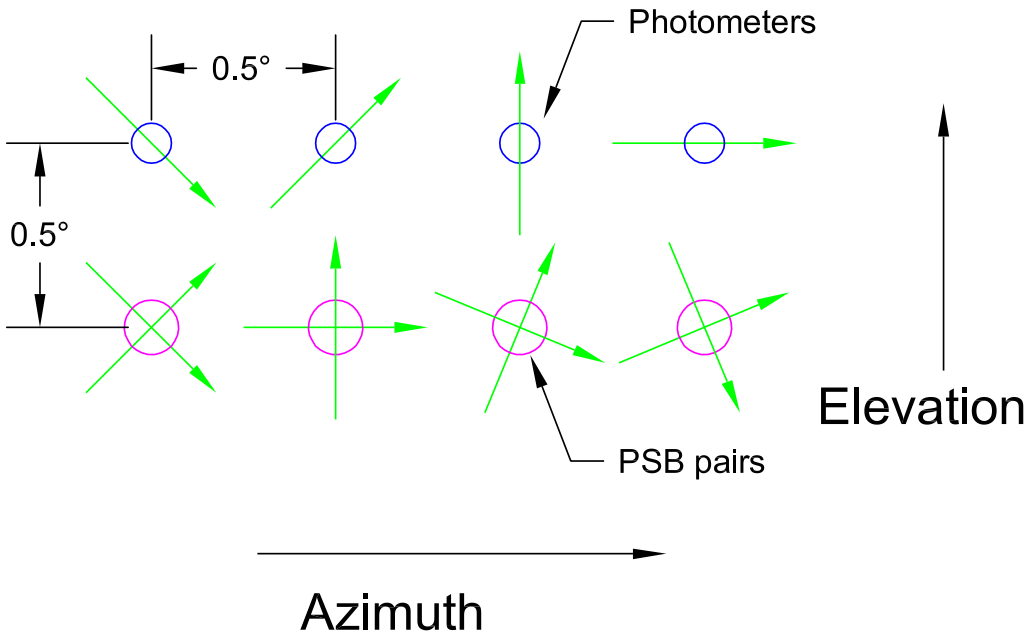

Fig. 3.— Focal Plane Schematic. 2-color photometers with band centers at 245 GHz and 345 GHz populate the upper row. Each photometer is only sensitive to one polarization. The lower row has 4 pairs of PSB's. The elements in a PSB pair are sensitive orthogonal polarizations. The circles representing the pixels show relative beams sizes: $\sim 7'$ for both photometer channels and $9'$ for the PSB's. The green arrows through the circles show the orientation of the polarization sensitivity. The photometer and PSB rows are separated by 0.5° in elevation, while the pixels in a row are separated by 0.5° in cross-elevation.

the same filters and feed structure.

Figure 5 shows the feed structure for a PSB pair. Light enters into a corrugated back-to-back feed horn, travels out of the back feed horn, across the thermal break and into the filter stack which is mounted on the front of the corrugated reconcentrating feed. The filter stack consists of metal mesh low pass filters which which define the upper edge of the band to be roughly 170 GHz and a Yoshinaga/Black-poly filter which prevents high frequency leaks. The lower edge of the band is defined by the waveguide cut-off of the back-to-back horn to be 122 GHz. Once the radiation passes through the filter stack, it enters the reconcentrating feed which couples the radiation to the pair of PSB's sitting at its exit aperture. The entire feed structure is designed so that polarization is preserved as the radiation travels from the entrance aperture to the bolometers (Jones et al. 2003).

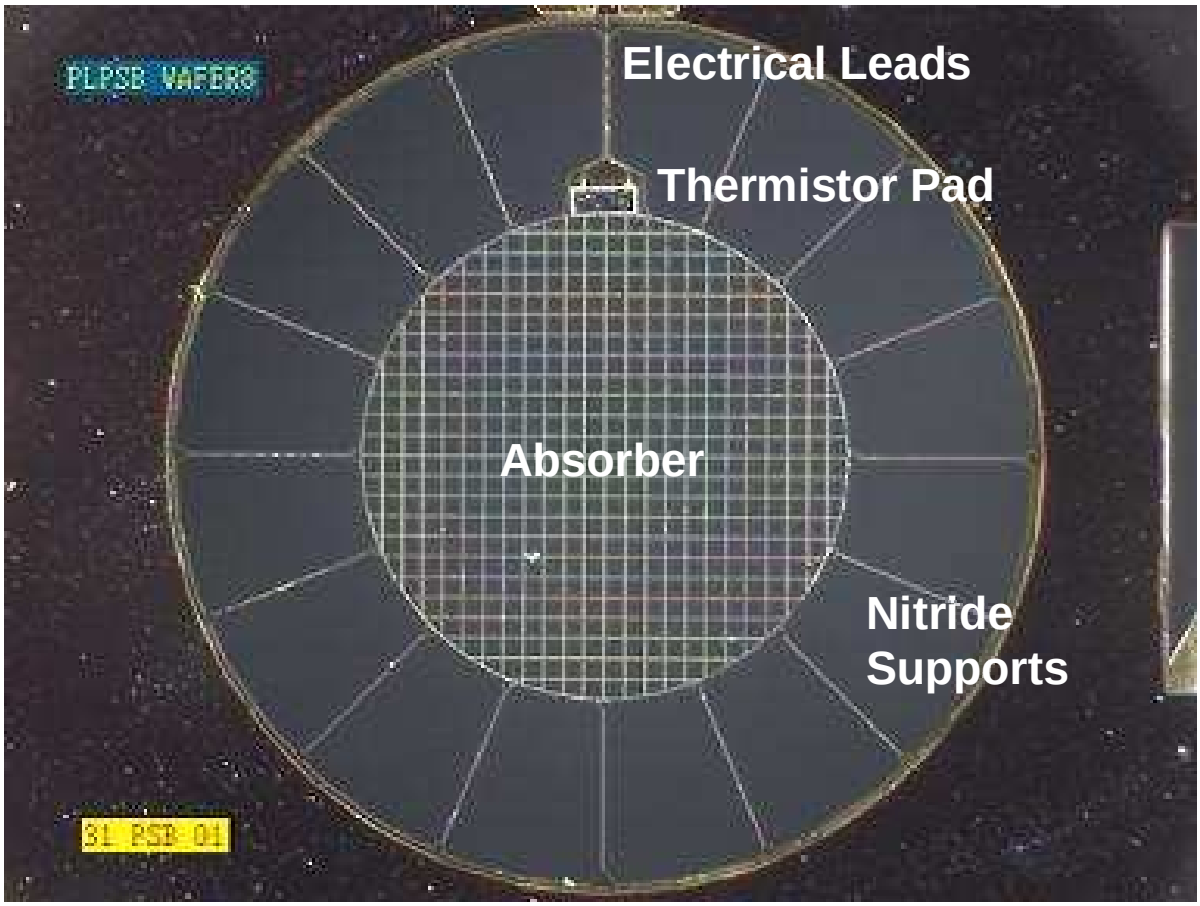

Fig. 4.— A Polarization Sensitive Bolometer. The diameter of the grid is 2.6 mm. The Si_3N_4 mesh is metallized in the vertical direction only, making the device sensitive to vertical polarization only. The horizontal component of the grid is un-metallized and provides mechanical support for the device. Orthogonally metallized devices are spaced 60μm apart at the exit aperture of a corrugated feed structure.

4. Photometers

The 2-color photometer (Figure 6) design has evolved from the 3-color photometer of B98. The photometers operate at 245 and 345 GHz using conventional spider web bolometers. It is fed by a back-to-back corrugated feed which was designed to be single-moded from 180 GHz to nearly 400 GHz. The photometers are made polarization sensitive by placing a polarizing grid in front of feed horn entrance aperture.

Incoming radiation passes through the polarizing grid and into the back-to-back feed horn. It exits the feed horn and enters the photometer body passing through a metal mesh low pass and a Yoshinaga/Black-poly filter. Radiation below 295 GHz is transmitted by the dichroic to the 245 GHz bolometer, and the high frequency radiation is reflected to the 345 GHz bolometer.

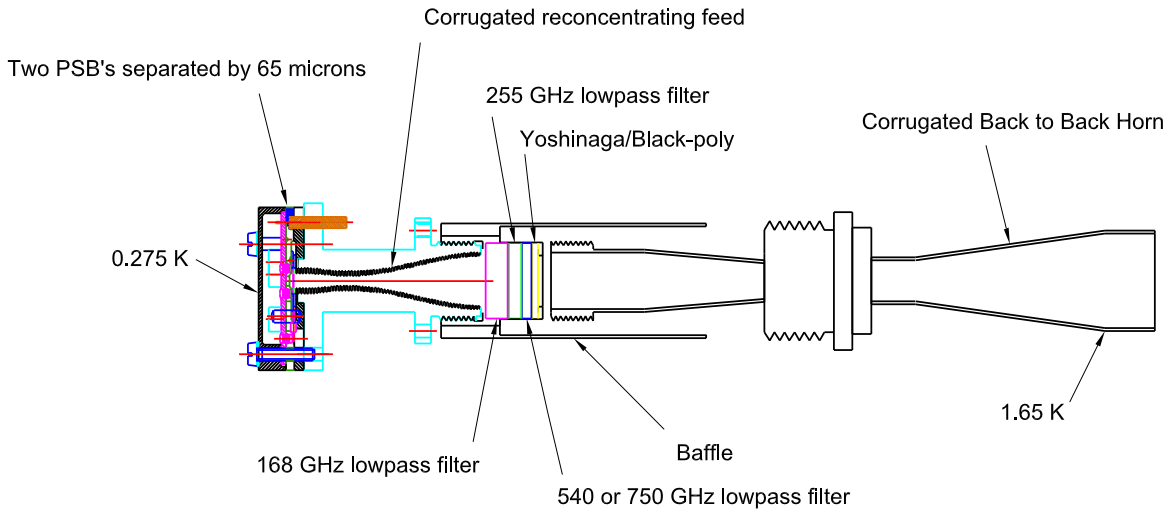

Fig. 5.— The PSB feed structure. Radiation travels through the back-to-back feed and passes through the filter stack as it enters the reconcentrating feed. The PSB pair sits at the exit aperture of the reconcentrating feed. Both the back-to-back feed and the reconcentrating feed are designed to preserve polarization.

5. Measuring Polarization

The Stokes parameters completely describe the polarization state of an electric field. A general polarized electromagnetic wave with angular frequency $\omega = 2\pi\nu$ can be described by:

$$\vec{E} = E_x(t)sin(\omega t - \delta_x(t))\hat{x} + E_y(t)sin(\omega t - \delta_y(t))\hat{y}. \quad (1)$$

The Stokes parameters can be written as

$$I = \langle E_y^2 + E_x^2 \rangle , \quad (2)$$
$$Q = \langle E_x^2 - E_y^2 \rangle , \quad (3)$$
$$U = \langle 2E_y E_x \cos(\delta_y - \delta_x) \rangle , \quad (4)$$
$$V = \langle 2E_y E_x \sin(\delta_y - \delta_x) \rangle , \quad (5)$$
$$\tau = \frac{1}{2} \tan^{-1}(\frac{U}{Q}), \quad (6)$$

where the averaging is done over times scales longer than the period of the wave. The total intensity of the radiation is described by I. Parameters Q and U describe the linear polarization, while V quantifies the degree of circular polarization ($V = 0$ when the radiation is linearly polarized). τ is the polarization angle.

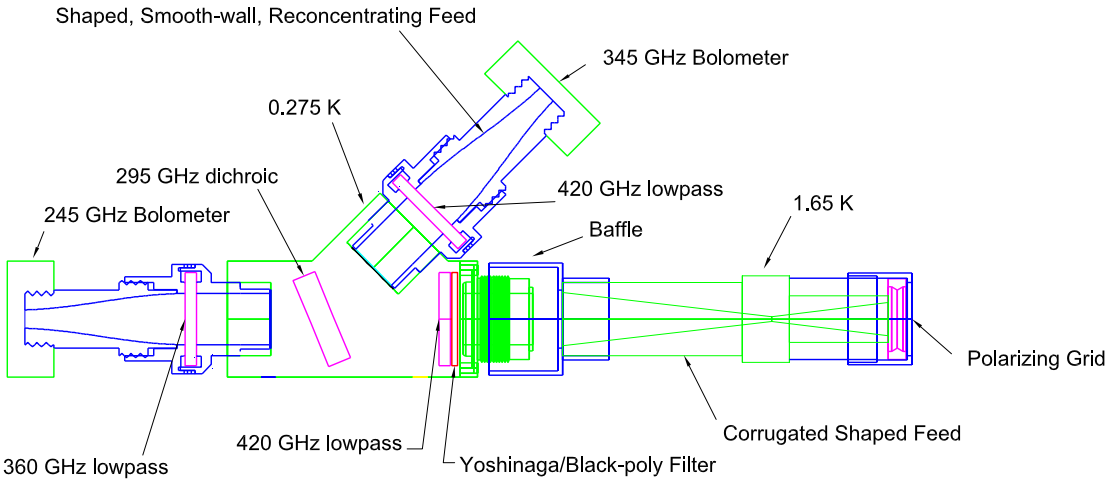

Fig. 6.— The photometer feed structure. Radiation passes through a polarizing grid mounted in front of the back-to-back feed horn. It exits the feed horn and enters the photometer body passing through a pair of low pass filters. A dichroic transmits frequencies below 295 GHz to the 245 GHz bolometer and reflects high frequency radiation to the 345 GHz bolometer.

Ideally, the signal from one of our detectors is comprised of the total power received in one polarization. For example, the signal received by a detector sensitive to the x-component of the electric field would be proportional to E_x^2. In order to measure Q and U, we must combine data from different detectors or multiple rotation angles for a single detector. This issue is complicated by the fact that each of our detectors has a finite cross-polarization $(1\% - 10\%)$ meaning that our x-polarized detector is contaminated with a small amount of E_y^2.

A single detector with no cross-polarization measures a combination I, Q and U in a pixel p. The signal is

$$V_i^p = \gamma_i(I^p + Q^p \cos(2\alpha) + U^p \sin(2\alpha)), \quad (7)$$

$$= \gamma_i T_i^p \quad (8)$$

where V_i is the detector voltage, α is the polarization orientation of the detector, γ_i is the calibration factor. I, Q and U are expressed as deviations from T_{CMB} and T_i^p is the total signal seen in one polarization. The calibration factor (with units V/K_{CMB}) is defined with respect to an unpolarized source. This is consistent with defining CMB temperature and polarization signals as

$$T = \frac{T_x + T_y}{2}, \quad (9)$$

$$Q = \frac{T_x - T_y}{2}. \quad (10)$$

The polarization efficiency can be described as the ratio of the signal in the desired polarization

to total signal, for example

$$\rho_x = \frac{2\gamma_x E_x^2}{V_x}, \tag{11}$$

where E_x^2 is the x-component of the incoming radiation and V_x is the signal measured by a detectors with polarization orientation in the $\hat{x}$ direction. If $\rho = 1$, there is no cross-polarization. If we rotate a polarized source in front of our detector, then the detector sees a signal

$$S = \beta(1 - \rho \sin^2(\theta_{det} - \theta_{source})), \tag{12}$$

where $S = \beta$ when the source and detector have aligned polarizations and $S = \beta(1 - \rho)$ when the source and detector are 90° apart.

To understand the effect of polarization efficiency, it is easiest to consider a PSB pair with polarizations oriented in the $\hat{x}$ and $\hat{y}$ directions. For the general case, we can apply the rotation rules for the Stokes parameters. Including the effects of cross polarization, we have

$$V_x = 2\gamma_x(E_x^2 + (1 - \rho_x)E_y^2), \tag{13}$$

$$V_y = 2\gamma_y(E_y^2 + (1 - \rho_y)E_x^2), \tag{14}$$

which can be re-written as

$$V_x = 2\gamma_x((1 - \frac{\rho_x}{2})I + \frac{\rho_x}{2}Q), \tag{15}$$

$$V_y = 2\gamma_y((1 - \frac{\rho_y}{2})I - \frac{\rho_y}{2}Q). \tag{16}$$

If we let $\rho_x = \rho_y = \rho$, then we get a rather simple solution

$$I = \frac{1}{2}\frac{\frac{V_x}{\gamma_x} + \frac{V_y}{\gamma_y}}{2 - \rho}, \tag{17}$$

$$Q = \frac{1}{2}\frac{\frac{V_x}{\gamma_x} - \frac{V_y}{\gamma_y}}{\rho}, \tag{18}$$

illustrating that the cross-polarization causes a loss of efficiency for Q measurement. Since the polarization signal is approximately 10% of the temperature anisotropy signal, the above equations illustrate the importance of high-precision measurements of the gains and polarization efficiencies for each channel.

6. BOOM03 Flight

The second long duration flight of BOOMERANG was launched on January 6, 2003 from Williams Field at McMurdo Station, Antarctica. The flight lasted for 15 days before it was terminated on January 21. During that time period, we were able to get 11.7 days of good data. We lost 20 hours because the ^{3}He refrigerator ran out at the end of day 11, and we had to recycle it. Also, the payload was losing altitude for most of the flight. At the end of day 13, we had to shutdown the telescope because wind shear at 70,000 ft made attitude control difficult.

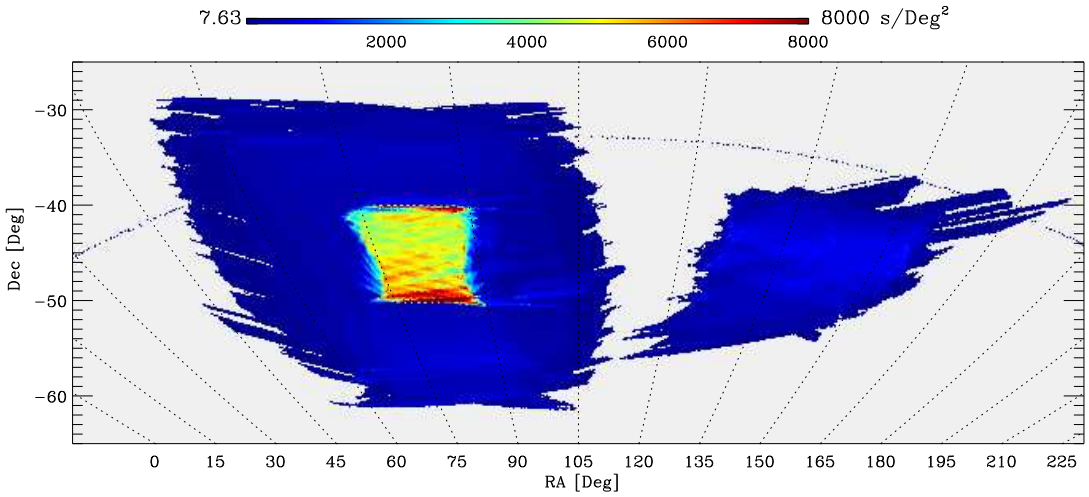

Fig. 7.— Sky coverage for one element of one PSB pair.

Even with the loss of altitude from 120,000 ft to 70,000 ft, the 145 GHz channels were not severely effected. At 75,000 ft, the 145 GHz channels had a responsivity which was approximately 15% less than the peak responsivity, while the 245 and 345 GHz channels had responsivities which were 30% less than their peak value. We did not dip below 95,000 ft until the end of day 11. At 95,000 ft, the 145 GHz channels had only a 5% responsivity loss, while the 245 and 345 GHz channels had a 10% loss.

The scan strategy was designed to balance the effects of sample variance and noise, optimizing our sensitivity to C_ℓ^T, C_ℓ^{TE} and C_ℓ^{EE}. Our entire CMB region covers an area of 1284 deg^2, slightly larger than the region used for B98 in Ruhl et al. (2002). This region was split into a shallow region of size 1161 deg^2 and a deep region of size 123 deg^2. We also spent time observing near the galactic plane in an attempt to characterize foreground polarization. Figure 7 shows a plot of the sky coverage for one 145 GHz detector and Table 2 shows how our observation time was divided.

Region	7' pixels	Area (deg^2)	Average Time (s)
CMB Deep	9397	123	46
CMB Shallow	88547	1161	3.35
CMB Total	97944	1284	7.45
Galaxy	29944	393	4.67

Table 2: A list of the BOOM03 primary scan regions, including the average amount of observation time per pixel per detector. The CMB Total region is the union of the CMB Shallow and CMB Deep regions; the average time per pixel is a bit skewed since the deep region pixels dominate the average.

7. Projected Results

With our flight data in hand, we can project our sensitivity to C_ℓ^T, C_ℓ^{TE}, and C_ℓ^{EE}. Figure 8 shows what we can expect statistically with eight detectors at 145 GHz. These error bars are estimated using the formulas presented in Zaldarriaga et al. (1997). The combined NET assumes that all channels have an $\mathrm{NET}_{CMB} = 160\mu K\sqrt{s}$. No allotment is made for calibration uncertainty, beam uncertainty, pointing error, systematics or the fact that long time constants at 145 GHz will decrease signal-to-noise at high-ℓ.

8. Acknowledgments

The BOOMERANG project has been supported by NASA, NSF-OPP and NERSC in the U.S., by PNRA, Universitá "La Sapienza" and ASI in Italy, by PPARC in the UK, and by CIAR and NSERC in Canada. T.M. acknowledges support from a NASA GSRP fellowship. The authors would like to thank the National Scientific Balloon Facility (NSBF) and the U.S. Antarctic Program for excellent field and flight support.

REFERENCES

B. P. Crill, et al. 2002, astro-ph/0206254, submitted to ApJ

J. H. Goldstein, et al. 2002, astro-ph/0212517, submitted to ApJ

G. Hinshaw, et al. 2003, astro-ph/0302217, submitted to ApJ

W. C. Jones, et al. "A Polarization Sensitive Bolometric Receiver for Observations of the Cosmic Microwave Background", in Proceedings of SPIE Vol. **4855** *Millimeter and Submillimeter Detectors for Astronomy*, edited by T.G. Phillips, J. Zmuidzinas, (SPIE, Bellingham, WA, 2003) page 227.

A. Kogut, et al. 2003, astro-ph/0302213, submitted to ApJ

J. M. Kovac, E. M. Leitch, C. Pryke, J. E. Carlstrom, N. W. Halverson, and W. L. Holzapfel. *Nature*, 420:772–787, December 2002.

C. L. Kuo, et al. 2002, astro-ph/0212289, submitted to ApJ

S. Masi et al., *Cryogenics*, 38:319, 1998.

S. Masi et al., *Cryogenics*, 39:217, 1999.

B. Mason, et al. 2002, astro-ph/0205384, ApJ in press

J. E. Ruhl, et al. 2002, astro-ph/0212229, submitted to ApJ

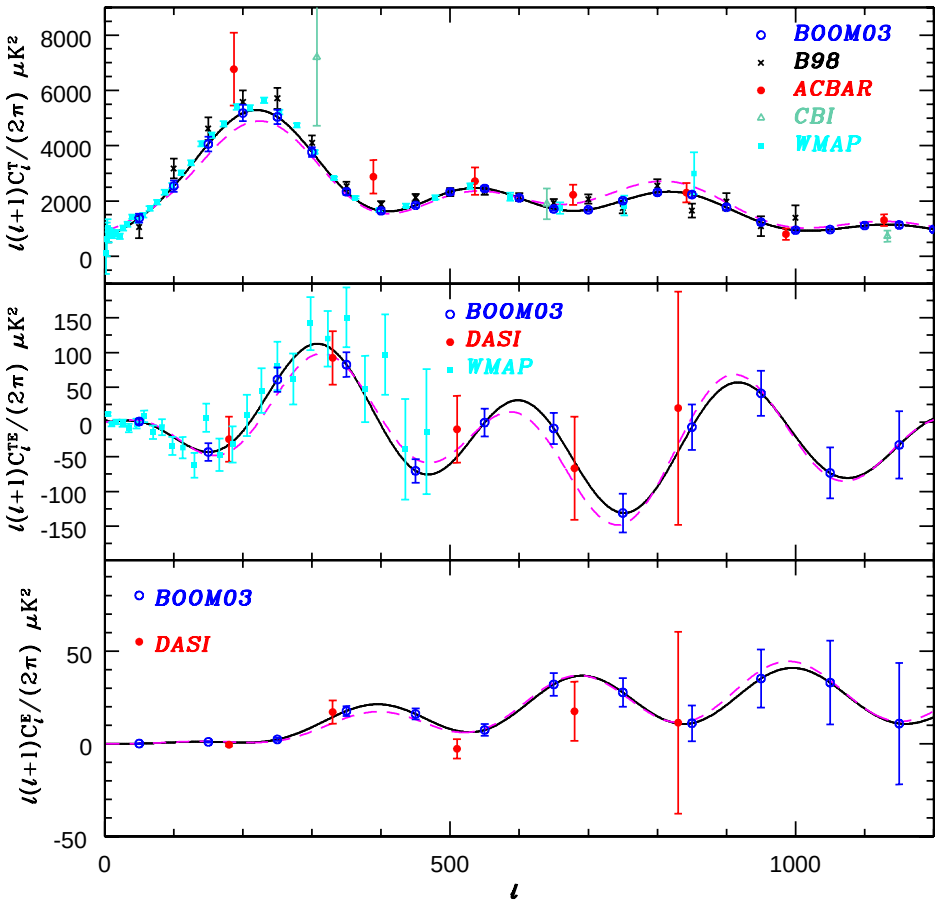

Fig. 8.— Forecasted results for BOOM03 at 145 GHz compared with recent results from B98 (Ruhl et al. 2002), ACBAR (Kuo et al. 2002), WMAP (Hinshaw et al. 2003), CBI (Mason et al. 2002) and DASI (Kovac et al. 2002). The top panel shows C_ℓ^T, the middle shows C_ℓ^{TE}, and the bottom C_ℓ^E. The models are best fits to the pre-WMAP data (Goldstein et al. 2002) for a ΛCDM model (black line) and a $\Lambda = 0$ model (dashed magenta line). This is a statistical calculation assuming that all 8 145 GHz channels have an $\mathrm{NET}_{CMB} = 160\mu K\sqrt{s}$. No allotment is made for calibration uncertainty, beam uncertainty, pointing error, systematics or the fact that our long time constants at 145 GHz will decrease signal-to-noise at high-ℓ.

M. Zaldarriaga, D. N. Spergel, and U. Seljak. ApJ, 488:1, October 1997.